Heliyon 6 (2020) e05463

Contents lists available at ScienceDirect

Heliyon

journal homepage: www.cell.com/heliyon

Research article

Up-regulation of PKR pathway contributes to L-NAME induced hypertension and renal damage

Jaspreet Kalra, Audesh Bhat, KirtiKumar B Jadhav, Arti Dhar *

Department of Pharmacy, Birla Institute of Technology and Sciences (BITS) Pilani, Hyderabad Campus, Jawahar Nagar, Shameerpet, Hyderabad, Telangana 500078, India

ARTICLE INFO

Keywords:
PKR
Renal complication
Mean arterial pressure
Renal inflammation
Fibrosis

ABSTRACT

Objective: Hypertension induced kidney damage is often associated with fibrosis and tubular apoptosis. Double-stranded protein kinase (PKR) is a well recognized inducer of inflammation and apoptosis. However, role of PKR in hypertension coupled renal damage is still not explored. Therefore here we sought to investigate the role of PKR in the pathogenesis of L-NAME induced hypertension and renal damage in Wistar rats and the underneath molecular mechanism.

Methods: L-NAME (40 mg/kg, p.o) and imoxin (0.5 mg/kg, i.p) was given to Wistar rats for 4 weeks. Increased eNOS expression, serum creatinine, BUN and changes in mean arterial pressure confirmed for hypertensive renal damage. Western blot and immunohistochemistry was carried out for PKR and markers for fibrosis and apoptosis. Morphological alterations were assessed by H&E staining. Sirius red and Masson's Trichrome staining was performed for collagen and fibrosis. TUNEL assay was done for tubular cell death and apoptosis.

Results: Increased expression of PKR and its downstream markers were reported in L-NAME rats, attenuation was observed with imoxin treatment. L-NAME treated rats showed a significant increase in MAP, serum calcium, creatinine and BUN along with the significant morphological changes, attenuation was reported with the imoxin treatment.

Conclusion: PKR is a core contributor in the pathogenesis of L-NAME induced renal damage and tubular apoptosis. Therapeutically targeting of PKR could be an attractive approach to treat the renal complications associated with hypertension.

1. Introduction

Impairment of renal function as a consequence of hemodynamic and cellular changes during hypertensive damage causes the replacement of functional nephrons by fibrotic lesions [1]. Increased activity of renin-angiotensin system (RAS) contributes to the pathogenesis of hypertension and renal injury [2, 3]. These diverse pathologies appear to incite a vicious cycle of swelling and inflammation resulting in a common pathophysiologic mechanism in which glomerular injury leads to interstitial inflammation, scarring and apoptosis [4]. Emerging evidence shows that angiotensin-II (Ang-II), one of the potent byproducts of RAS activation is not only a vasoactive peptide, but also a true cytokine and a key mediator of hypertension associated kidney damage that regulates reactive oxygen species (ROS), cell growth, inflammation and fibrosis [5, 6, 7]. Ang-II in-vivo causes increase in the production of tumor necrosis factor-a (TNF-α) and other pro-inflammatory mediators such as nuclear factor kappa-light-chain-enhancer of activated B cells (NF-κB), c-Jun N-terminal kinases (JNK) activation and mitogen-activated protein kinases (MAPKs) pathways which are associated with the presence of glomerular and interstitial inflammatory cells in the kidney [8, 9]. Ang-II/NF-κB and TGF-β1 signaling pathways are closely related with inflammation and fibrosis development due to their capacity to promote the recruitment of inflammatory cells into glomerulus as well as into the tubulointerstitium. Activation of these pathways further leads to the synthesis of extracellular matrix (ECM) proteins and inhibitors that inhibit the effect of proteases involved in degradation of ECM [10, 11].

Double-stranded protein kinase, PKR is a recognized inducer of inflammation, oxidonitrosative stress and apoptosis. PKR activates inflammatory signaling cascade through activation of NF-κB and JNK causing fibrosis and cellular apoptosis [12, 13, 14]. Previous studies have successfully demonstrated the role of PKR in obesity and type 2 diabetes disease models [15, 16, 17]. Inflammation, oxidative stress and apoptosis are interconnected in the development of hypertension. However, no studies have been done so far to explore the role of PKR in hypertension

* Corresponding author.
E-mail address: artidhar@hyderabad.bits-pilani.ac.in (A. Dhar).

https://doi.org/10.1016/j.heliyon.2020.e05463
Received 3 August 2020; Received in revised form 28 September 2020; Accepted 4 November 2020

related renal damage. Previously, we have reported the association of PKR in endothelial dysfunction, cardiovascular remodeling and renal inflammation [18, 19]. In continuation with our previous study, we establish the role of PKR in NG-Nitro-L-arginine Methyl Ester, Hydrochloride (L-NAME) induced renal damage. Therefore, this study we elucidated *(i)* Pathogenic involvement of PKR signaling in hypertensive renal damage using L-NAME-induced hypertension; *(ii)* Pathomorphologic changes associated with PKR activation that comprise renal inflammation, fibrosis and its underneath mechanism; *(iii)* The effects of PKR activation on tubular cell death.

2. Material and methods

2.1. Chemicals

PKR specific inhibitor C16 (imoxin), Nω-Nitro-L-arginine methyl ester hydrochloride (L-NAME hydrochloride), poly-L-lysine solution (0.1 % w/v in H_2O), Bicinchonic acid assay kit (BCA-1), 4′,6-diamidino-2-phenylindole (DAPI), RIPA buffer, Protease inhibitor, Phenyl methyl sulfonyl fluoride Eosin, hematoxylin, luminal, and p-Coumaric acid were purchased from Sigma Aldrich (St. Louis, MO, USA). TUNEL assay kit and Masson's trichrome kit were purchased from Abcam (Milton, Cambridge, UK). Commercial kits for assessment of serum creatinine, blood urea nitrogen, (BUN) were purchased from Arkray Health care Pvt. Ltd, Surat, Gujrat, India. Dpx mountant media (Ref:Lamb/Dpx).

2.2. Antibodies

Primary antibodies for anti-α-smooth-muscle actin, protein kinase R, caspase-3, JNK, p-JNK (G-7), NF-Ķb, $ERK_{1/2,}$ Angiotensinogen (H-12), Renin (B-12), eNOS (A-9), TGF-β, TNF-α (52B83), β-actin and goat anti-mouse IgG-HRP were procured from Santa Cruz Biotechnology (Santa Cruz, California, USA). Antibody for advance glycation end products was procured from Abcam, R&D, Minneapolis, MN 55413, USA. Secondary antibody for texas red goat anti rabbit and alexa flour 488 goat-anti mouse were procured from Invitrogen, Thermo fisher scientific CA, USA.

2.3. Experimental rats

Male Wistar rats, n = 8 were randomly allocated to four groups. Rats not weighing less than 180–230 g and eight weeks old were used in the present study. Experimental rats were purchased from registered CPCSEA breeders. Laboratory conditions were maintained as following temperature (22 ± 1 °C), relative humidity (55–60%). 12 h light/dark cycle was maintained throughout rats were given excess to water ad libitum and food. Animals were familiarized to laboratory conditions for 7 days. Measurements for blood pressure (non-invasive) were recorded between 9:00 and 17:00 h. Experimental protocol (BITS/HYD/IAEC/2016706) was approved by Institutional Animal Ethical Committee (IAEC), Birla Institute of Technology and Science Pilani, Hyderabad Campus. We hereby confirm that all the experiments were performed in accordance with the guidelines issued by Committee for the Purpose of Control and Supervision of Experiments on Animals (CPCSEA), Ministry of Social Justice and Environment, Government of India. Directive 2010/63/EU of the European Parliament on the protection of animals used for scientific purposes and Animal Research: Reporting of In-Vivo Experiments (ARRIVE) guidelines were also followed for animal care and for preparing this manuscript.

2.4. L-NAME treatment and experimental protocol

L-NAME (40 mg/kg b.w, p.o) and imoxin ((C16) 0.5 mg/kg, i.p) was given for four weeks. Dose selection for L-NAME and imoxin were based on previously reported literature [17, 20]. Animals were divided into four groups with n = 8 rats in each group: Group I: Control (CON), Group II: L-NAME, Group III: L-NAME + C16 (40 mg/kg, p.o+0.5 mg/kg, i.p), Group IV: C16 (0.5 mg/kg, i.p).

2.5. Non-invasive blood pressure (BP) measurement

Mean arterial pressure (MAP) was measured in awakened rats in each group on weekly basis. Rats were acclimatized and habituated to rat restrainer for 15 min/day for 7 consecutive days before the actual BP recordings. 10 recordings for MAP were made for each rat using the MRBP system (IITC Life Science, Woodland Hills, CA). Average of nearby/approximate values of six measurements for each animal was considered for the graphical presentation.

2.6. Biochemical estimations

Following MAP measurement animals were anesthetized with (1.5–2% isofluorane, 2 L/min oxygen flow rate), blood samples were collected, and colorless to whitish yellow serum supernatant was isolated. Serum creatinine and BUN were carried out for biochemical estimations. On 28^{th} day kidneys were harvested and stored for further experiments. After confirmation of unconsciousness anesthetized animals were sacrificed by cervical dislocation.

2.7. Biochemical estimations

Serum creatinine, BUN and serum calcium were measured by assay kits according to the manufacturer's instructions.

2.8. Relative kidney weight: an indicator for assessing kidney hypertrophy

Following sacrifice, both the kidneys were isolated and harvested. Kidneys were de-capsulated, and washed with saline for two times. Kidneys were dried and weighed. Kidney hypertrophy was determined using kidney to body weight ratio [21].

2.9. Western blot

Protein was isolated from Kidney tissue homogenates. Obtained protein samples were quantified by using the bicinchoninic acid assay (BCA). 40 μg of protein samples were loaded on 8–10% of the SDS page. Membranes were blocked either with 5% non-fat milk or 3% BSA for 1h at room temperature and incubated overnight with primary antibody (1:1000 dilutions) at 4 °C. The membranes were washed thrice with PBS-T, 15 min for each period and incubated with secondary antibody (1:2000 dilutions) for 2 h. The membrane was washed thrice, immunoreactivity to desire protein was detected with the help of an Enhanced Chemiluminescence Reagent. Direct and indirect markers for inflammation and vasoconstriction: Angiotensinogen, Renin, NF-ķB, JNK, p-JNK, and TNF-α. Markers for fibrosis and apoptosis: TGF-β, α-smooth muscle actin (α-SMA) $ERK_{1/2}$, and caspase 3. Blots for TNF-α and α-SMA were from same membrane. Blots of JNK and TGF-β also share the same B-actin as they were also ran on the same membrane.

2.10. Immunohistochemistry: confocal laser scanning microscopy for PKR and associated markers

Immunohistochemistry was carried out according to the method described previously [20]. Briefly, 4μm sections were used. Sections were fixed in ice-cold acetone, air-dried for 30 min and washed with PBS. Blocking was done with 3% BSA followed by overnight incubation with primary antibody at 4 °C using 1:200 dilutions of PKR, eNOS, renin, angiotensinogen, and AGEs antibody. Sections were incubated with fluorescent labeled secondary antibody (1:2000 dilutions) for 2 h, stained with nuclear dye DAPI for 10 min followed by washing with PBS-T. Cover slips were placed. 20X magnification was used for confocal

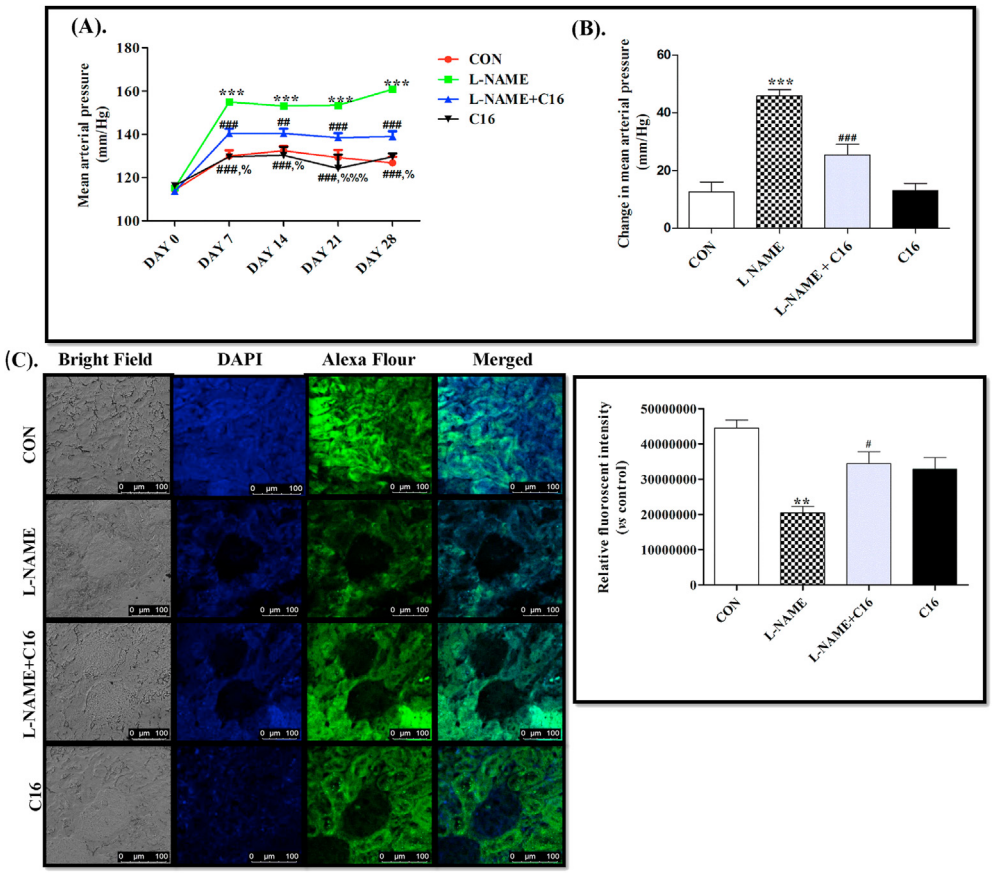

Figure 1. Induction of experimental hypertension, associated kidney damage and attenuation by imoxin (C16): (A) Represents measurement of MAP in each experimental group (B) Shows alterations in initial and final MAP. (C) Increased expression of renal eNOS in L-NAME rats, improvement by imoxin. Statistical analysis was carried out by applying one-way ANOVA/two-way ANOVA, Bonferroni test was used for post hoc analysis.

imaging (Leica DMi8, Leica Microsystems, Germany). 10X magnification was used for imaging sections stained for AGEs. Settings were kept constant throughout each individual experimental group.

2.11. Histology: H&E staining

H&E staining was performed according to the method described previously [20]. 40X magnification and bright field microscopy were used. Images were captured using an upright microscope (Carl Zeiss microscopy, Germany). Analysis was performed by the individual who was blind to the study. Tubular atrophy and glomeruli sclerotic index was quantified by the method as described by Ninichuk et al. [22, 23].

2.12. Picro sirius red staining for fibrosis and Masson's trichrome staining for \ collagen deposition

5μm sections were sliced. Tissue slicing was dried overnight at 55 °C. Slicing was deparaffinized and hydrated. Briefly, 200 μl of picro-sirius stain was applied and sections were incubated for 1 h at room temperature. Slides were washed twice with 0.5% acetic acid, followed by washing. Lastly, sections were dipped twice in 100% alcohol and mounted. Instructions to manufacturer were followed for Masson's trichrome staining. Blue deposits indicate collagen accumulation. Imaging was done at 40X magnification using an upright microscope (Carl Zeiss microscopy, Germany).

2.13. In situ detection of DNA strand breaks: TUNEL assay for cellular apoptosis

To quantitate nuclei with fragmented DNA deoxynucleotidyl transferase (TUNEL) assay was performed according to the manufacturer's instruction. Paraffin-embedded sections (4μm) were cut onto a glass slide. Sections were rehydrated with dips of xylene followed by changes in decreasing concentration of ethanol. Sections were permeabilized with proteinase K and quenching was done for endogenous peroxidases. Samples were equilibrated, labeled with deoxynucleotidyl transferase

Table 1. Estimation of Serum creatinine and blood urea nitrogen (BUN): Statistical analysis was carried out by applying one-way ANOVA, Bonferroni test was used for post hoc analysis.

EXP GP	Serum Cr (mg/dl)		Serum BUN (mg/dl)	
	DAY 0	DAY 28	DAY 0	DAY 28
CON	0.67 ± 0.0723	0.79 ± 0.0374	0.46 ± 0.0867	0.42 ± 0.0629
L-NAME	0.69 ± 0.0948	1.41 ± 0.7467***	0.48 ± 0.0725	1.57 ± 0.4664***
L-NAME + C16	0.72 ± 0.0875	0.84 ± 0.1004#	0.41 ± 0.0722	1.17 ± 0.4525#
C16	0.69 ± 0.074	0.72 ± 0.1123	0.42 ± 0.1080	0.59 ± 0.0711

***p<0.001 vs Control; #p<0.05 vs L-NAME group.

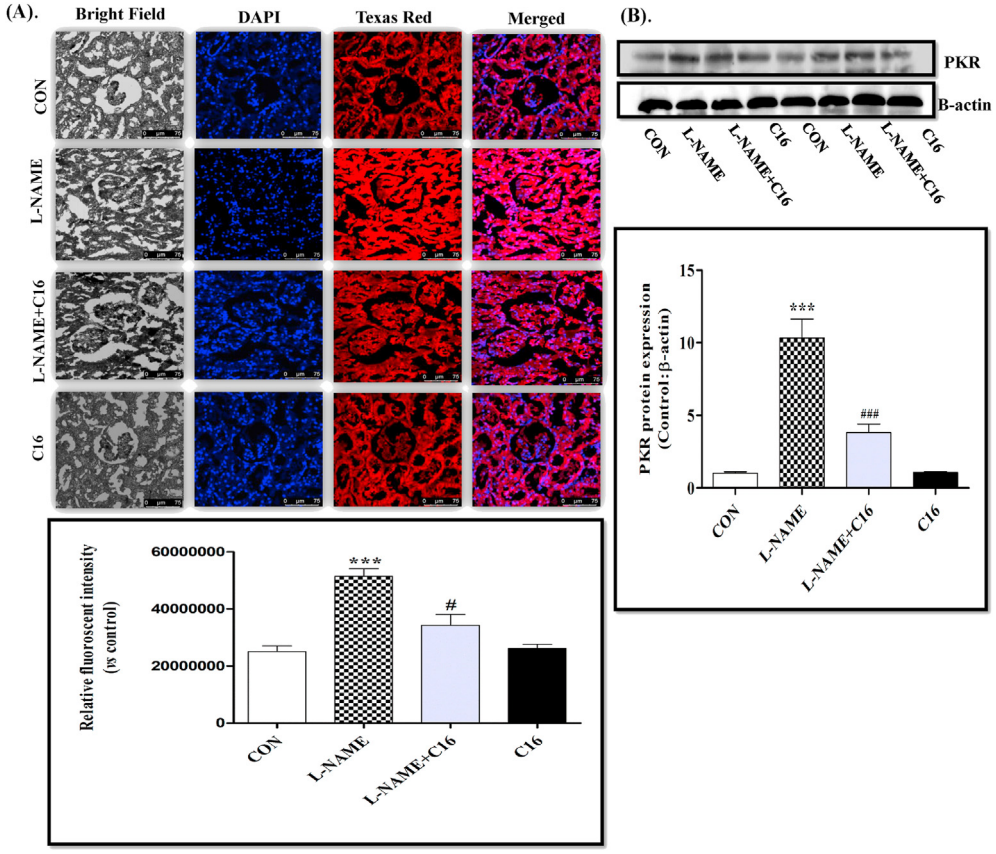

Figure 2. Increased PKR expression in L-NAME-treated rats and restoration by imoxin (C16): (A) Increased PKR expression in LNAME rats, inhibition by imoxin. (B) Western blot reveals significant increase in PKR expression in L-NAME rats compared to CON rats, inhibition by imoxin. Statistical analysis was carried out by applying one-way ANOVA, Bonferroni test was used for post hoc analysis.

(TdT) enzyme for 1.5 h at room temperature. The reaction was ended by adding stop buffer and slides were washed with tris buffer saline (TBS) followed by blocking. Slides were developed by adding a working diaminobenzidine (DAB) solution. Finally, the slides were counter-stained with methyl green and incubated at room temperature for 1–3 min. Slides were dipped in two changes of 100% ethanol and cover slips were placed. Images were visualized at 40X magnification using the Zeiss microscope (Carl Zeiss microscopy, Germany).

2.14. Statistical analysis

Data is presented as mean ± S.E.M, n relates to number of samples. One way/two way analysis of variance (ANOVA), Bonferroni's post hoc test was used for statistical analysis. The P-value$</ = 0.05$ was considered significant. Statistical analysis was carried out by using Graph Pad Prism version 5 software, (San Diego, California, USA). *Data expressed as mean ± SEM: *P < 0.05, **P < 0.01, ***P < 0.001 vs. CON, #P < 0.05, ##P < 0.01, ###P < 0.001 vs. L-NAME + C16 treated group.*

3. Results

3.1. Development of experimental hypertension in L-NAME treated rats, inhibition by imoxin

Significantly increased MAP, change in MAP (Figure 1A & B), serum creatinine and BUN (Table1) along with the reduced expression of eNOS (Figure 1C), were noted in the L-NAME group compared with the control group, improvement was observed with imoxin treatment. Alterations in these parameters suggested chronic renal impairment due to the development and progression of hypertension.

3.2. Imoxin attenuates PKR in L-NAME treated rat kidney

Figure 2A, B, reveals increase in renal PKR expression in L-NAME treated rats, inhibition was reported with imoxin.

3.3. Imoxin improves L-NAME triggered RAS activation facilitates renin and angiotensinogen expression in rat kidney

Next, we aimed to look whether PKR activation can cause angiotensinogen up regulation or not. Present findings reveals up regulation in renal angiotensinogen (Figure 3A & B), and renin (Figure 3C & D), in L-NAME treated rats whereas significant down regulation was reported with the imoxin.

3.4. Imoxin attenuates L-NAME induced tubulointerstitial fibrosis, phenotypic transition by inhibition of TGF-β in rat kidney

TGF-β is a significant promoter of enhancing ECM synthesis. It is an essential paramount that contributes to glomerulosclerosis and interstitial fibrosis. AGEs are also known to promote fibrosis via enhancement of ECM deposition [24]. We report increased fibrosis in renal tubules and glomerulus (Figure 4A), along with the substantial increase in TGF-β expression (Figure 4B) in L-NAME treated rats. However, we observed considerable improvement in fibrosis with imoxin treatment. We relate this improvement with TGF-β inhibition. Elevated α-SMa expression

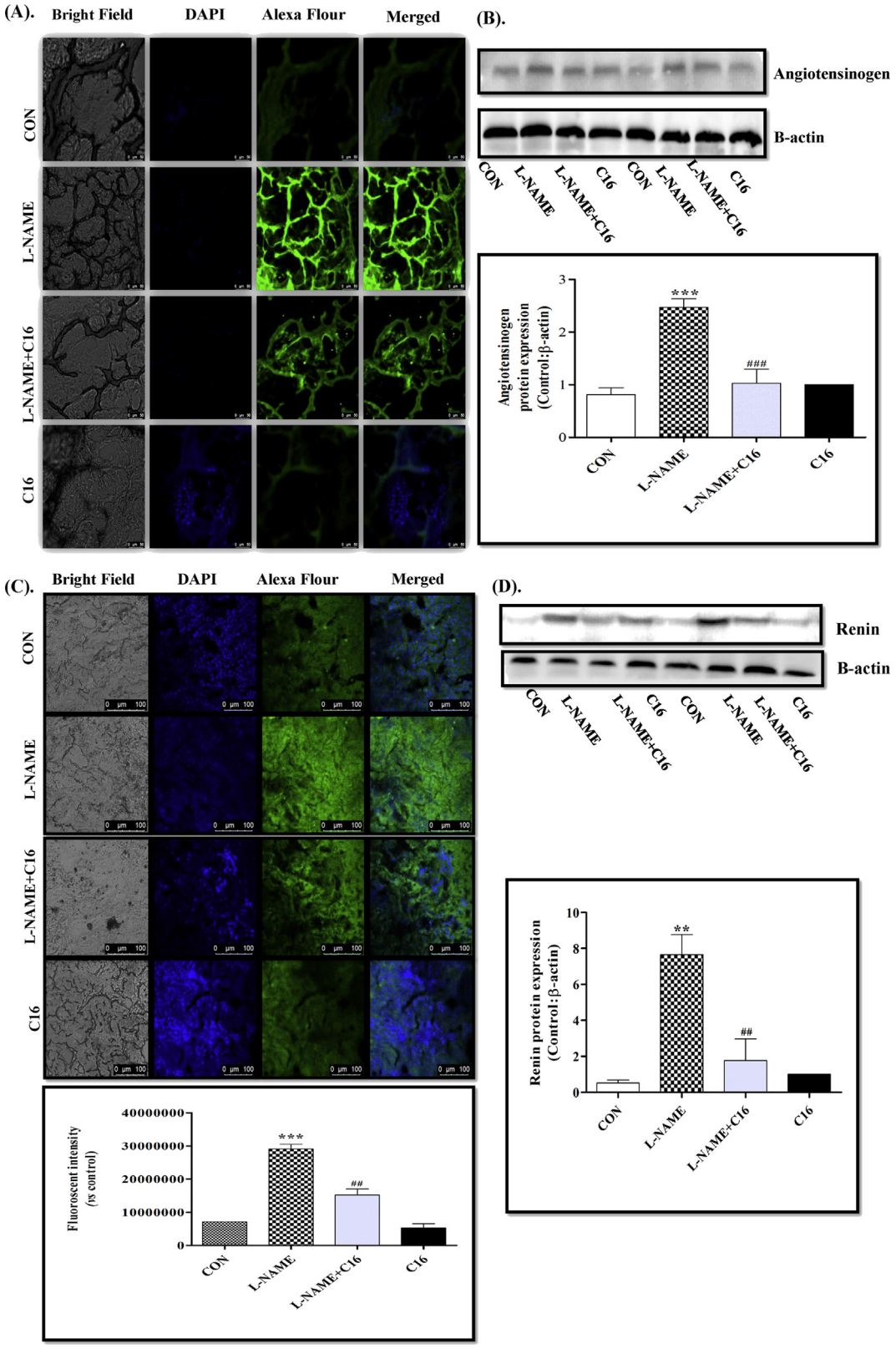

Figure 3. Angiotensinogen and renin expression is increased in LNAME-treated rats, attenuation by imoxin (C16): (A) Up regulation in expression of angiotensinogen in L-NAME rats compared to CON rats, inhibition by imoxin (B) Up regulation in angiotensinogen protein in L-NAME rats compared to CON rats, inhibition by imoxin. (C) Up regulation in expression of renin in L-NAME rats compared to CON, attenuation by imoxin. (D) Up regulation in renin protein expression in L-NAME rats compared to CON rats, inhibiion by imoxin. Statistical analysis was carried out by applying one-way ANOVA, Bonferroni test was used for post hoc analysis.

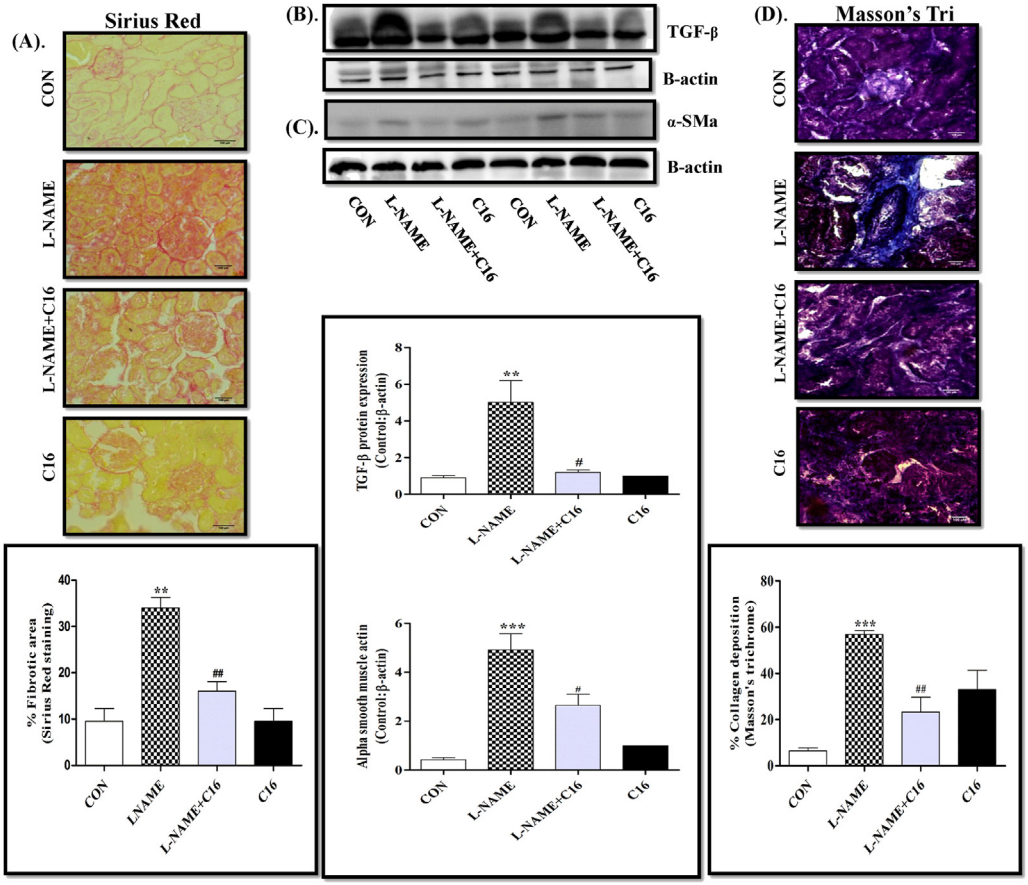

Figure 4. Imoxin attenuates L-NAME induced tubulointerstitial fibrosis, phenotypic transition by inhibition of TGF-β in rat kidney: (A) Assessment of tubulointerstitial fibrosis. Increased fibrosis was noted in L-NAME rat's vs CON, inhibition with imoxin. (B) Up regulation in TGF-β protein expression: a characteristic marker of fibrosis and collagen accumulation. Up regulation in TGF-β expression in L-NAME-treated rats, inhibition by imoxin. (C) Significant rise in expression of α-smooth muscle actin (α-SMa) in L-NAME rats, an indicator of fibroblastic transition into myofibroblasts, inhibition by imoxin. (D) Excessive collagen deposition in kidney of L-NAME rats. Higher collagen deposition is shown by blue coloration deposits in L-NAME rats, inhibition by imoxin. Statistical analysis was carried out by applying one-way ANOVA, Bonferroni test was used for post hoc analysis Data is presented as mean ± SEM.

(Figure 4C), and excessive collagen accumulation (*blue deposits,* (Figure 4D)) was observed in kidney samples of L-NAME treated rats, we report inhibition with imoxin.

3.5. Imoxin inhibits L-NAME evoked inflammatory responses and expression of AGEs

Present findings show that L-NAME treatment evokes an inflammatory response in rat kidney, as demonstrated by increased protein expression of p-JNK (Figure 5A), JNK (Figure 5B), attenuation was observed with imoxin treatment. Substantial increase in the activity of NF-ķB (Figure 5C), TNF-α (Figure 5D) and AGEs (Figure 5E) in L-NAME treated rats followed by its attenuation with imoxin was also reported in the present study.

3.6. Imoxin improves L-NAME induced morphological changes

Next, we sought to investigate structural and morphological alterations in kidneys of L-NAME administered rats. Higher incidence of glomerulosclerosis and tubular dilation in was seen in L-NAME treated rats (Figure 6A & B), compared to control, improvement was observed with imoxin. Extensive hypertrophy was reported in L-NAME rats compared to control, we report inhibition with imoxin (Figure 6C).

3.7. Imoxin attenuates L-NAME associated tubular cell apoptosis by inhibition of $ERK_{1/2}$, caspase-3

L-NAME treated rat exhibits significantly elevated protein expression of $ERK_{1/2}$ and caspase-3 in L-NAME rats. In addition to this significant cellular apoptosis and apoptotic glomeruli were also reported in L-NAME treated rat kidney compared to control, where as attenuation was observed with imoxin treatment (Figure 7C, B, & A).

3.8. Imoxin improves L-NAME induced increased calcium levels and nephrocalcification

Ang-II directly exerts its effect on raising serum calcium release along with the activation of MAPKs followed by oxidative stress and apoptosis. Based on this assumption we stained L-NAME treated rat kidney sections with alizarin red stain and measured serum calcium level. Result indicates higher number of calcification centers along with the elevations in serum calcium in L-NAME rats, improvement was observed with imoxin (Figure 8A & B).

4. Discussion

We are the first to report that inhibition of PKR by imoxin (Figure 2A & B), attenuates hypertension associated tubulointerstitial fibrosis and cellular apoptosis in L-NAME treated rats by partial improvement of angiotensinogen/TGF-β through inhibition of PKR. We observed chronic inhibition of NOS by L-NAME in wistar rats induces hypertension (Figure 1). Increase in MAP (Figure 1A and B), in L-NAME rats signifies experimental hypertension, attenuation was reported with imoxin. Elevated serum creatinine, and BUN (Table.1) indicates hypertension induced renal damage, improvement was observed with imoxin. Further, we also report substantial reduction in renal eNOS in L-NAME administered rats, restoration in renal eNOS was noted with imoxin treatment (Figure 1C).

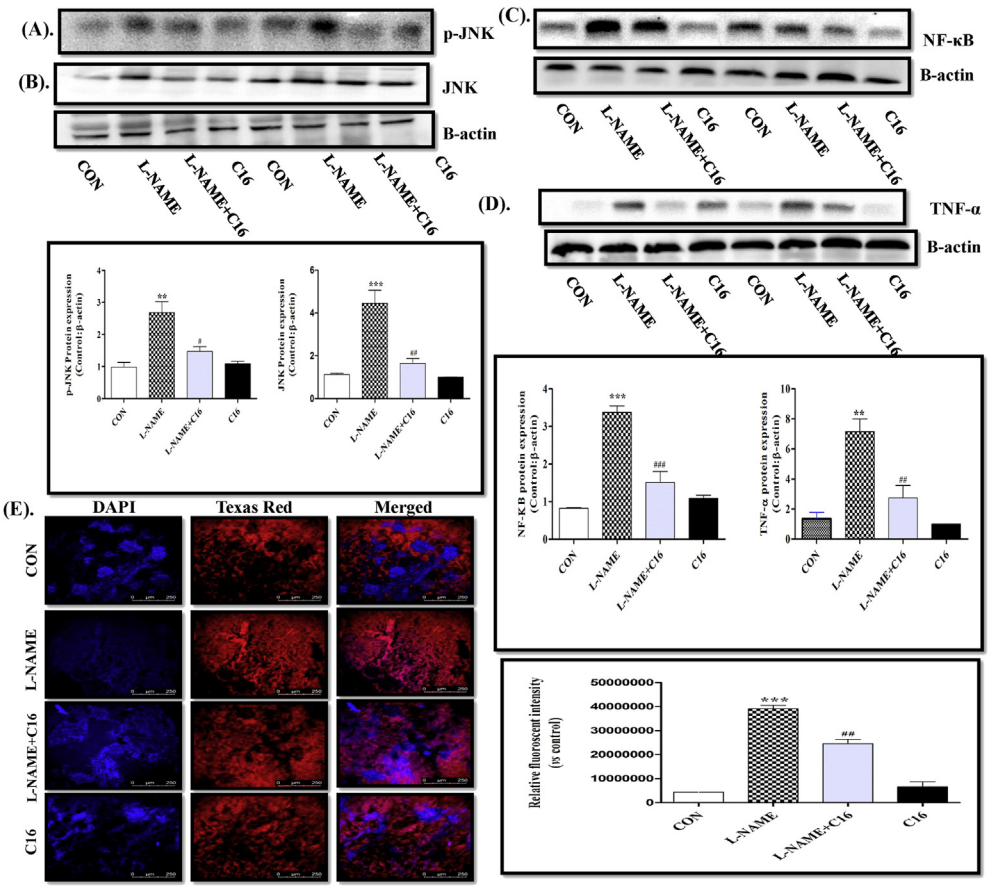

Figure 5. L-NAME up regulates inflammatory responses and expression of AGEs in rat kidney, attenuation by imoxin: A Elevated p-JNK expression in L-NAME rats, inhibtion by imoxin. B Up regulation in JNK expression in L-NAME- rats, inhibition by imoxin. C Elevated NF-ķB expression in L-NAME rats, inhibition by imoxin. (D) Elevated TNF-α protein in L-NAME rats, inhibition by imoxin. E Up regulation in expression of AGEs in L-NAME rats compared to CON rats, inhibition by imoxin. Statistical analysis was carried out by applying one-way ANOVA, Bonferroni test was used for post hoc analysis.

In-vivo Ang-II activates renal NF-κB pathway via up-regulation of several pro-inflammatory genes initiating a local inflammatory response [6, 25, 26, 27]. In our study, we report for the first time upregulation of angiotensinogen in kidney of L-NAME rats and its inhibition by selective PKR inhibitor imoxin (Figure 3).

PKR is a crucial contributor in mediating inflammatory cascade through activation of NF-κB and MAPKs. Members of MAPKs such as extracellular regulated kinase1/2 ($ERK_{1/2}$), and JNK regulates cellular proliferation and apoptosis [28]. NF-κB up regulation and pathogenic involvement of JNK is correlated in renal diseases [29]. We found that PKR caused significant increase in angiotensinogen and renin in L-NAME treated rats (Figure 3A & B and C & D), improvement was witnessed with imoxin treatment. Increase in p-JNK, JNK, NF-κB and TNF-α (Figure 5A, and B), attenuation was also seen with imoxin in L-NAME treated rats. NF-κB and TNF-α (Figure 5C & D), increase in renal tissue could be associated with the initiation of local inflammatory responses [12].

Next, we aimed to look for PKR associated tubulointerstitial fibrosis in hypertension induced kidney damage. Ang-II promotes the deposition of ECM by augmented release of endogenous profibrotic growth factors such as TGF-β [8, 29, 30, 31, 32]. In the discussed study L-NAME treated rat kidney showed remarkable hypertrophy (Figure 6C), up-regulation of TGF-β (Figure 4B), and increased collagen deposition (Figure 4D), however, significant inhibition was observed with imoxin treatment.

α-SMA is one of the prominent marker to signify enhanced tubulointerstitial fibrosis [33, 34]. In our study, L-NAME administered rats' exhibit remarkable tubulointerstitial fibrosis shown by activated angiotensinogen/TGF-β pathway. Sirius red staining visualizes the significant fibrosis ((Figure 4A) *increased red coloration deposits in renal tubules and glomeruli*), whereas (Figure 4C), shows increase in α-SMA in L-NAME administered rats, significant reduction in renal fibrosis and α-SMA expression was seen with imoxin treatment.

Patients with glomerular sclerosis and proliferative glomerulonephritis present an increased number of apoptotic glomeruli. Apoptotic glomeruli are characterized by active caspase-3 rich DNA strand fragments. Increased caspase-3 (Figure 7C), and TUNEL positive tubular and glomeruli cells were observed in L-NAME treated rats (Figure 7D), attenuation was observed with imoxin treatment. Tubular cells are considered as the vital contributors involved in interstitial fibrosis and scarring [35, 36]. Findings of histological examination further reveal significant morphological changes such as increased glomerulosclerosis and tubular dilation in L-NAME treated rats, reversal was observed with imoxin treatment (Figure 6A). We hypothesize that the observed morphological alterations in the L-NAME administered rat kidney could be attributed to the activation of MAPKs in a PKR dependent manner. We also report nephroclacification in L-NAME rats, zero calcification centers were seen with imoxin treatment (Figure 7A). Increased calcium deposits in L-NAME group could be possibly due to the elevated serum calcium levels augmented by over activated angiotensinogen in a PKR dependent pathway. We suggest that further studies should be carried out for exploring the exact mechanism.

According to Arany et al., NRK-52E cells challenged with cisplatin undergo cellular apoptosis through EGFR/Src/ERK-dependent mechanisms, with no role of JNK in tubular cell death [37]. Contrary to this report authors of the same group have also reported the protective role of $ERK_{1/2}$ in response to H_2O_2 mediated cellular death. Further, they also proposed that over activated JNK activity is held accountable for cell death and toxicity [38, 39, 40]. However, in contrast to both the reports we found increased expression of p-JNK, JNK as well as for $ERK_{1/2}$, however, attenuation was observed p-JNK, JNK (Figure 5A & B), $ERK_{1/2}$ (Figure 7B), and AGEs (Figure 5E) with imoxin in L-NAME rats. Therefore, in light of the above experimental evidences we propose that L-NAME induces substantial hypertension and renal damage through a

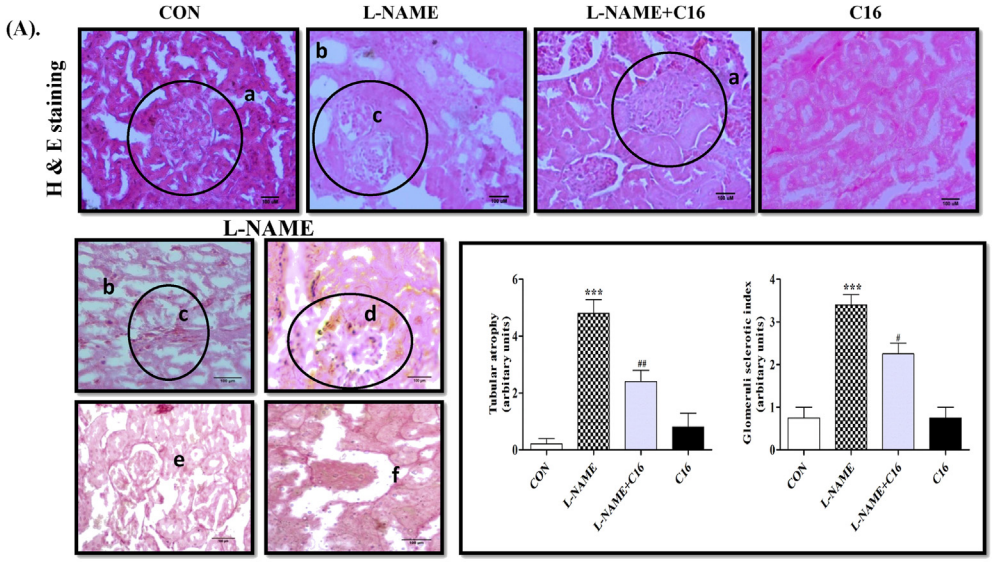

a: Normal glomeruli, b: Tubular atrophy, c: Glomerulosclerosis, d: Collapsed glomeruli

e: Tubular necrosis, f:Dilation in renal corpuscles

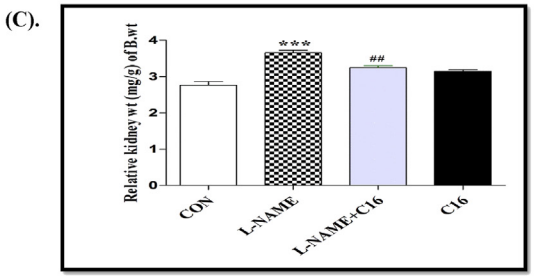

Figure 6. Imoxin attenuates L-NAME induced tubular atrophy, glomerulosclerosis and kidney hypertrophy: (A) H&E staining indicates significant tubular atrophy in kidney sections of L-NAME rats, inhibition by imoxin. (B) Higher occurence of glomerulosclerosis was noted in kidney sections of L-NAME rats inhibition by imoxin (C) Represents relative kidney weight: preliminary indicator for kidney hypertrophy in L-NAME rats, inhibition by imoxin. Statistical analysis was carried out by applying one-way ANOVA, Bonferroni test was used for post hoc analysis.

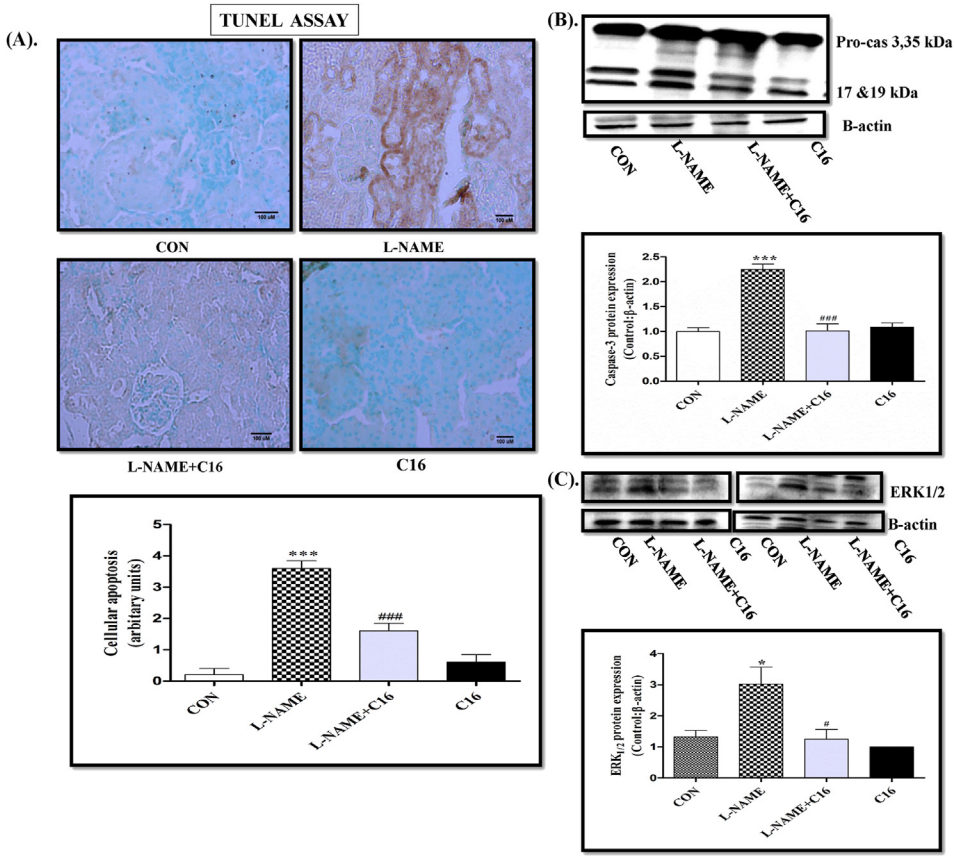

Figure 7. L-NAME triggered up-regulation of $ERK_{1/2}$ and cellular apoptosis, attenuation by imoxin: (A) Increased cellular apoptosis was noted in TUNEL assay in L-NAME rat kidney, inhibition by imoxin. (B) Elevated expression of caspase 3 in L-NAME rat kidney, inhibition by imoxin. (C) Elevated $ERK_{1/2}$ in L-NAME rat kidney, inhibition by imoxin. Statistical analysis was carried out by applying one-way ANOVA, Bonferroni test was used for post hoc analysis Data is presented as mean ± SEM: *P < 0.05, **P < 0.01, ***P < 0.001 vs. CON, #P < 0.05, ##P < 0.01, ###P < 0.001 vs. L-NAME + C16 treated group.

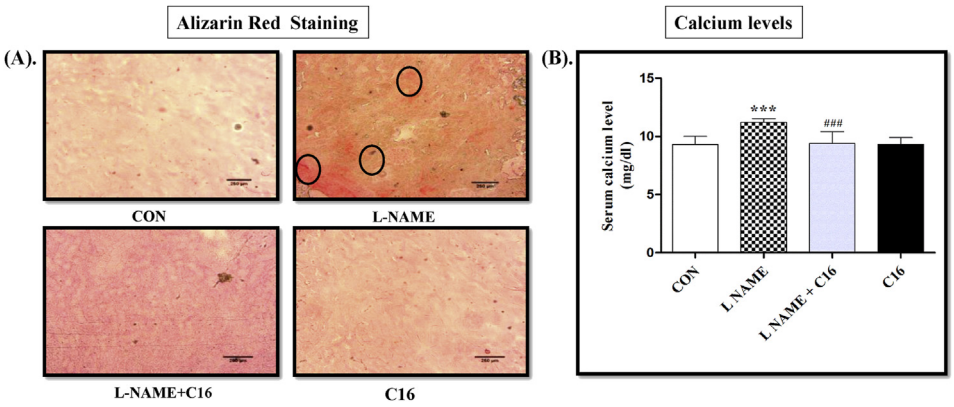

Figure 8. L-NAME triggered nephro-calcification and attenuation by imoxin: (A) Alizarin red staining: nephro-calcification was noted in L-NAME rat kidney, inhibition by imoxin. (B) Elevated serum calcium level in L-NAME rats, inhibition by imoxin.

marked up regulation of angiotensinogen/TGF-β in a PKR related manner. Successful reversal of hypertension and improvement in morphological changes were achieved through the PKR inhibition with imoxin in L-NAME administered rats. Therefore, we present PKR as a potential target for hypertension and related renal complications.

Declarations

Author contribution statement

A. Dhar: Conceived and designed the experiments; Contributed reagents, materials, analysis tools or data; Wrote the paper.
J. Kalra: Performed the experiments; Wrote the paper.
A. Bhat: Conceived and designed the experiments.
KirtiKumar B. Jadhav: Analyzed and interpreted the data.

Funding statement

Jaspreet Kalra received fellowship from Council for Scientific and Industrial Research (CSIR-JRF), India.

Declaration of interests statement

The authors declare no conflict of interest.

Additional information

No additional information is available for this paper.

References

[1] S. Mennuni, S. Rubattu, G. Pierelli, G. Tocci, C. Fofi, M. Volpe, Hypertension and kidneys: unraveling complex molecular mechanisms underlying hypertensive renal damage, J. Hum. Hypertens. 28 (2014) 74–79.
[2] A. Toke, T. Meyer, Hemodynamic effects of angiotenin II in the kidney, in: G. Wolf (Ed.), The Renin-Angiotensin System and Progression of Renal Diseases, first ed., Karger, Basel, 2001, pp. 34–46.
[3] V.M. Vehaskari, T. Stewart, D. Lafont, C. Soyez, D. Seth, J. Manning, Kidney angiotensin and angiotensin receptor expression in prenatally programmed hypertension, Am. J. Physiol. Ren. Physiol. 287 (2004) F262–F267.
[4] G. Remuzzi, T. Bertani, Pathophysiology of progressive nephropathies, N. Engl. J. Med. 339 (1998) 1448–1456.
[5] M. Ruiz-Ortega, O. Lorenzo, Y. Suzuki, M. Rupérez, J. Egido, Proinflammatory actions of angiotensins, Curr. Opin. Nephrol. Hypertens. 10 (2001) 321–329.
[6] M. Ruiz-Ortega, M. Rupérez, V. Esteban, J. Rodríguez-Vita, E. Sánchez-López, G. Carvajal, et al., Angiotensin II: a key factor in the inflammatory and fibrotic response in kidney diseases, Nephrol. Dial. Transplant. 21 (2006) 16–20.
[7] C. Rüster, G. Wolf, Angiotensin II as a morphogenic cytokine stimulating renal fibrogenesis, J. Am. Soc. Nephrol. 22 (2011) 1189–1199.
[8] G. Wolf, F.N. Ziyadeh, F. Thaiss, J. Tomaszewski, R.J. Caron, U. Wenzel, et al., Angiotensin II stimulates expression of the chemokine RANTES in rat glomerular endothelial cells. Role of the angiotensin type 2 receptor, J. Clin. Invest. 100 (1997) 1047–1058.
[9] F.Y. Ma, R.S. Flanc, G.H. Tesch, Y. Han, R.C. Atkins, B.L. Bennett, et al., A pathogenic role for c-Jun amino-terminal kinase signaling in renal fibrosis and tubular cell apoptosis, J. Am. Soc. Nephrol. 18 (2007) 472–484.
[10] P.M. Tang, Y.Y. Zhang, T.S. Mak, P.C. Tang, X.R. Huang, H.Y. Lan, Transforming growth factor-β signalling in renal fibrosis: from Smads to non-coding RNAs, J. Physiol. 596 (2018) 3493–3503.
[11] S. Kagami, W.A. Border, D.E. Miller, N.A. Noble, Angiotensin II stimulates extracellular matrix protein synthesis through induction of transforming growth factor-beta expression in rat glomerular mesangial cells, J. Clin. Invest. 93 (1994) 2431–2437.
[12] G.R. Stark, I.M. Kerr, B.R. Williams, R.H. Silverman, R.D. Schreiber, How cells respond to interferons, Annu. Rev. Biochem. 67 (1998) 227–264.
[13] A. Kumar, J. Haque, J. Lacoste, J. Hiscott, B.R. Williams, Double-stranded RNA-dependent protein kinase activates transcription factor NF-kappa B by phosphorylating I kappa B, Proc. Natl. Acad. Sci. U. S. A. 91 (1994) 6288–6292.
[14] J. Couturier, M. Morel, R. Pontcharraud, V. Gontier, B. Fauconneau, M. Paccalin, et al., Interaction of double-stranded RNA-dependent protein kinase (PKR) with the death receptor signaling pathway in amyloid beta (Abeta)-treated cells and in APPSLPS1 knock-in mice, J. Biol. Chem. 28 (2010) 1272–1282.
[15] Y. Asakura, Y. Fujiwara, N. Kato, Y. Sato, T. Komatsu, Serine/threonine kinase PKR: a sentinel kinase that discriminates a signaling pathway mediated by TLR4 from those mediated by TLR3 and TLR9, Am. J. Hematol. 82 (2007) 640–642.
[16] T. Nakamura, M. Furuhashi, P. Li, H. Cao, G. Tuncman, N. Sonenberg, et al., Double-stranded RNA-dependent protein kinase links pathogen sensing with stress and metabolic homeostasis, Cell 140 (2010) 338–348.
[17] T. Nakamura, A. Arduini, B. Baccaro, M. Furuhashi, G.S. Hotamisligil, Small-molecule inhibitors of PKR improve glucose homeostasis in obese diabetic mice, Diabetes 63 (2014) 526–534.
[18] J. Kalra, S.B. Mangali, A. Bhat, I. Dhar, M.P. Udumula, A. Dhar, Imoxin attenuates high fructose-induced oxidative stress and apoptosis in renal epithelial cells via downregulation of protein kinase R pathway, Fundam. Clin. Pharmacol. 32 (2018) 297–305.
[19] J. Kalra, S. Mangali, A. Bhat, K. Jadhav, A. Dhar, Selective inhibition of PKR improves vascular inflammation and remodelling in high fructose treated primary vascular smooth muscle cells, Biochim. Biophys. Acta (BBA) - Mol. Basis Dis. 1866 (2020) 165606.
[20] J. Kalra, D. Dasari, A. Bhat, S. Mangali, S.G. Goyal, K.B. Jadhav, A. Dhar, PKR inhibitor imoxin prevents hypertension, endothelial dysfunction and cardiac and vascular remodelling in L-NAME-treated rats, Life Sci. 262 (2020) 118436.
[21] R.J. Fern, C.M. Yesko, B.A. Thornhill, H.S. Kim, O. Smithies, R.L. Chevalier, Reduced angiotensinogen expression attenuates renal interstitial fibrosis in obstructive nephropathy in mice, J. Clin. Invest. 103 (1999) 39–46.
[22] V. Ninichuk, A.K. Khandoga, S. Segerer, P. Loetscher, A. Schlapbach, L. Revesz, A. Khandoga, F. Krombach, P.J. Nelson, Schlöndorff, H.J. Anders, The role of interstitial macrophages in nephropathy of type 2 diabetes, Am. J. Pathol. 170 (2007) 1267–1276.
[23] V. Ninichuk, S. Clauss, O. Kulkarni, et al., Late onset of Ccl2 blockade with the Spiegelmer mNOX-E36-3'PEG prevents glomerulosclerosis and improves glomerular filtration rate in db/db mice, Am. J. Pathol. 172 (3) (2008) 628-637.
[24] B. Folkow, G. Göthberg, S. Lundin, S.E. Ricksten, Structural "resetting" of the renal vascular bed in spontaneously hypertensive rats (SHR), Acta Physiol. Scand. 100 (1977) 270–272.
[25] J.M. Bohlender, S. Franke, G. Stein, G. Wolf, Advanced glycation end products and the kidney, Am. J. Physiol. Ren. Physiol. 289 (2005) F645–F659.
[26] H. Pavenstädt, W. Kriz, M. Kretzler, Cell biology of the glomerular podocyte, Physiol. Rev. 83 (2003) 253–307.
[27] M. Ruiz-Ortega, O. Lorenzo, M. Rupérez, J. Blanco, J. Egido, Systemic infusion of angiotensin II into normal rats activates nuclear factor-kappaB and AP-1 in the kidney: role of AT(1) and AT(2) receptors, Am. J. Pathol. 158 (2001) 1743–1756.
[28] V. Esteban, M. Ruperez, J.R. Vita, E.S. López, S. Mezzano, J.J. Plaza, et al., Effect of simultaneous blockade of AT1 and AT2 receptors on the NFkappaB pathway and renal inflammatory response, Kidney Int. Suppl. 86 (2003) S33–S38.

[29] V. Esteban, O. Lorenzo, M. Rupérez, Y. Suzuki, S. Mezzano, J. Blanco, et al., Angiotensin II, via AT1 and AT2 receptors and NF-kappaB pathway, regulates the inflammatory response in unilateral ureteral obstruction, J. Am. Soc. Nephrol. 15 (2004) 1514–1529.
[30] Z. Xu, W. Li, J. Han, et al., Angiotensin II induces kidney inflammatory injury and fibrosis through binding to myeloid differentiation protein-2 (MD2), Sci. Rep. 7 (2017) 44911.
[31] K. Grynberg, F.Y. Ma, D.J. Nikolic-Paterson, The JNK signaling pathway in renal fibrosis, Front. Physiol. 8 (2017) 829.
[32] A. Fogo, V. Kon, Treatment of hypertension, Semin. Nephrol. 16 (1996) 555–566.
[33] L.K. Lee, T.W. Meyer, A.S. Pollock, D.H. Lovett, Endothelial cell injury initiates glomerular sclerosis in the rat remnant kidney, J. Clin. Invest. 96 (1995) 953–964.
[34] K. Tamaki, S. Okuda, M. Nakayama, T. Yanagida, M. Fujishima, Transforming growth factor-beta 1 in hypertensive renal injury in Dahl salt-sensitive rats, J. Am. Soc. Nephrol. 7 (1996) 2578–2589.
[35] S. Meran, R. Steadman, Fibroblasts and myofibroblasts in renal fibrosis, Int. J. Exp. Pathol. 92 (2011) 158–167.
[36] I. Loeffler, G. Wolf, Transforming growth factor-β and the progression of renal disease, Nephrol. Dial. Transplant. 29 (Suppl 1) (2014) i37–i45.
[37] J.R. Schelling, Tubular atrophy in the pathogenesis of chronic kidney disease progression, Pediatr. Nephrol. 31 (2016) 693–706.
[38] T. Suzuki, M. Kimura, M. Asano, Y. Fujigaki, A. Hishida, Role of atrophic tubules in development of interstitial fibrosis in microembolism-induced renal failure in rat, Am. J. Pathol. 158 (2001) 75–85.
[39] I. Arany, J.K. Megyesi, H. Kaneto, P.M. Price, R.L. Safirstein, Cisplatin-induced cell death is EGFR/src/ERK signaling dependent in mouse proximal tubule cells, Am. J. Physiol. Ren. Physiol. 287 (2004) F543–F549.
[40] I. Arany, J.K. Megyesi, H. Kaneto, S. Tanaka, R.L. Safirstein, Activation of ERK or inhibition of JNK ameliorates H(2)O(2) cytotoxicity in mouse renal proximal tubule cells, Kidney Int. 65 (2004) 1231–1239.